Information Sciences 532 (2020) 125–138

Contents lists available at ScienceDirect

Information Sciences

journal homepage: www.elsevier.com/locate/ins

Asynchronous control strategy for semi-Markov switched system and its application

Meng Li[a,b,*], Yong Chen[a,b], Longyu Xu[a,b], Zhang-yong Chen[a,b]

[a] School of Automation Engineering, University of Electronic Science and Technology of China, Chengdu, 611731, China
[b] Institute of Electric Vehicle Driving System and Safety Technology, University of Electronic Science and Technology of China, Chengdu, 611731, China

ARTICLE INFO

Article history:
Received 2 January 2020
Revised 30 March 2020
Accepted 3 April 2020
Available online 7 May 2020

Keywords:
DC-DC converter
Semi-Markov switched system
Uncertainty
External disturbance
Asynchronous control

ABSTRACT

In this paper, the problem of modeling and control for DC-DC converter is investigated. A novel switched system model is established and an asynchronous control strategy is designed. Firstly, the DC-DC converter is modeled by the semi-Markov switched system with uncertainty and external disturbance. In which, the change of resistance parameter and the jump of input voltage are considered. Additionally, the sojourn-time of the switch is considered in the new model, in this way, it can be more accurately to depict the dynamic behavior of the plant. Then, in order to guarantee the stability of the plant, a state feedback asynchronous controller is proposed. Furthermore, the stability conditions of the closed-loop system with a prescribed $H\infty$ index factor are given and the controller gains are solved. Finally, a numerical simulation and a practical experiment are executed to verify the superiority of proposed control strategies.

1. Introduction

Recently, since the merit in terms of high output power, good stability, high conversion efficiency and voltage booster, dc-dc converter has become the preferred power supply system in portable electronic products powered by batteries. The boost converter is the commonly applied topology of DC-DC converter, in recent years, the modeling and control for DC-DC converter has become a hot topic. Generally, it is difficult to apply the linear system method to model the converter duo to the characteristic of strong nonlinear [8]. Conventional, the averaging strategies are utilized to model the DC-DC converter, for example, state-space averaged model [1], which ignores the switching details. Hence, this method is simple, but the accuracy of the linearized model is required to within one fifth of the switching frequency [10]. Different from traditional averaged model, in this paper, a switched system ideal based on semi-Markov stochastic process is proposed for modeling DC-DC converter.

Markov jump systems (MJSs) can effectively characterize the dynamical of physical systems which suffer from abrupt changes, faults or variations and stochastic switching [6,17,22,26]. Hence, it has been widely employed in many practical plants, for instance, fault detection and networked control system [9,19], and so on. It is noticed that the sojourn time, is defined as the interval of arbitrary two jumps, is a stochastic variable and obeys by the exponential distribution for continuous-time situation. As a consequence, the transition rate is a constant because of the exponential distribution

* Corresponding author.
E-mail addresses: Lmengxhu@163.com (M. Li), ychencd@uestc.edu.cn (Y. Chen).

https://doi.org/10.1016/j.ins.2020.04.004
0020-0255/

owns the property of memoryless [10]. Therefore, this condition is too restrictive. Usually, in practice, the transition rate is time-varying. For example, Huang and Shi in [5] presented a bathtub curve which indicates the sojourn-time is time-varying (including: decrease, constant and increase). Hence, aiming at the sojourn time, a more popular distribution is brought.

In order to solve above-mentioned issue, a popular distribution is brought to describe the sojourn time, that is, the semi-Markov jump systems (S-MJSs) are proposed. Different from MJSs, the sojourn time in S-MJSs is not necessarily obeys an exponential distribution in continuous-time system. That is, the transition probabilities of the S-MJSs are dynamic and own the memory property. Hence, it can effectively model the general stochastic jumping systems. It is noted that the MJSs are the special case of the S-MJSs. In past few decades, S-MJSs have become hot research. In [20], for the continuous-time S-MJSs with uncertain, in order to ensure the stochastic stability of the plant, an output-feedback sliding mode controller is designed. In [12], considered the discrete-time S-MJSs with limited sojourn time, the stability issues of the plants are studied, and the approach based on semi-Markov kernel is designed to deal with this problem. In [14], an approximation method based on the Kalman-Bucy filter is proposed and applied it to S-MJSs, and the merit of the presented method lies on that it makes pre-computations possible. In [23], Zhang et al. developed the stability of discrete-time S-MJSs, the results indicate that when the distribution of sojourn-time is same in each mode, the different parameters and distributions can also be coexisted. In [24], Zhang and Li investigated the stability of hybrid linear parameter-varying plants, where the S-MJSs are employed to model the switching phenomenon. In [7], the singular plants with semi-Markov jumping is considered, the issue of robust sliding mode control (SMC) is studied. A common sliding surface is presented to alleviate the effect of jumping. In [25], it is assumed that the sojourn time of S-MJSs suffers from the exponentially modulated periodic probability, and the authors address the problems of stability of the system. In [15], Shen et al. discussed the discrete-time S-MJSs with slow sampling singular perturbations, and a feedback control method based on slow state variable is proposed to achieve the stability of plant. In [6], for the nonlinear S-MJSs with delay, a reduced-order adaptive SMC is designed. So far, although the research on S-MJSs has made some initial achievements, it also needs to further develop its theory and expand its application field.

Usually, asynchrony is ubiquitous between the controller mode and system mode duo to the widely existing delays or packet loss when transmitting data [2,21]. Hence, the survey of asynchronous control has caused the researcher's great concern in recent few years. In [3], for continuous-time nonlinear MJSs, it is assumed that the controller modes are asynchronously with the system modes, and the strictly dissipative control problem is studied. In [16], aiming at the MJS with time-delay, in which both the quantizer and controller are asynchronous with the plant, and an asynchronous state feedback controller is designed. In [18], Song et al. investigated asynchronous SMC for a kind of MJSs with stochastic perturbation and time-varying delays, and a hidden Markov model is employed to characterize the controller modes and system modes. Generally, in asynchronous control, the system modes are asynchronous with the controller modes, and both of them are contacted through a conditional probability. In this way, it can more accurate describe the actual system. Although the asynchronous control issue has been frequently concerned during the past few years, however, it is worth noting that the asynchronous control strategy for DC-DC converter with uncertainty and external disturbance has not been investigated. In particular, since the introduction of uncertainty and external disturbance in the switched systems, the design and synthesis of the asynchronous controller are more complicated and interesting, this motivates the presented work.

In this paper, the stability of the DC-DC converter is studied, and an asynchronous control strategy is presented. Specifically, First of all, the S-MJS is employed to depict the DC-DC converter plant, where the vary of resistance parameter and the jump of input voltage are simultaneous considered as the parameter uncertainty of system and external disturbance, respectively. Second, a state feedback asynchronous controller is presented in order to ensure the stability of the DC-DC converter. Thirdly, the stability conditions of the closed-loop system are given in form of the linear matrix inequality and the controller gains are solved.

The rest of this paper is organized as follows. Section 2 formulates the control problem and models the DC-DC converter based on semi-Markov. The stability conditions of the plant are presented and the asynchronous controller is designed in Section 3. Section 4 illustrates the superiority of designed control strategies. In Section 5, the conclusions are summarized.

Notations: "$*$"denotes the symmetric term in symmetric entries, and $Sym\{Z\}$ refers to $Z + Z^T$.

2. Problem formulation and semi-Markov modeling

2.1. Problem statement

Usually, there are two sates for the boost DC-DC converter operated at continuous conduction mode (CCM), that is, (a) Switch on. (b) Switch off. It is assumed the sampling period is T, then the plant will work under two states in each period, i.e., t_{on} and $t_{off} = T - t_{on}$, where t_{on} and t_{off} are the time of switch on and switch off, respectively. The boost DC-DC converter is shown in Fig. 1, in which, Fig. 1(a) denotes the circuit work under the switch on, and Fig. 1(b) presents the circuit work under the switch off.

The dynamic model of the DC-DC converter under the two work states can be described by

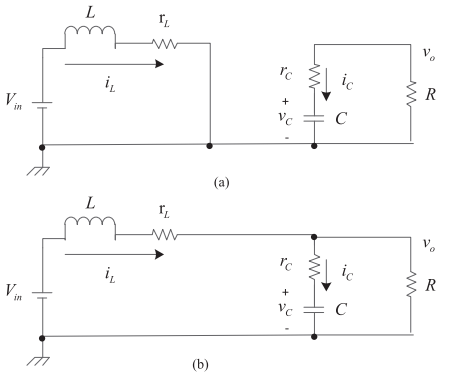

Fig. 1. Boost DC-DC converter. (a) Switch on. (b) Switch off.

(a) Switch on

$$\begin{cases} V_{in} = L\frac{di_L}{dt} + i_L r_L \\ i_C = C\frac{dv_C}{dt} \\ v_C = -i_C(R + r_C) \\ v_o = v_C + r_C i_C \end{cases} \tag{1a}$$

(b) Switch off

$$\begin{cases} V_{in} = L\frac{di_L}{dt} + i_L r_L + v_o \\ i_C = C\frac{dv_C}{dt} \\ i_L = i_C + \frac{v_o}{R} \\ v_o = v_C + r_C i_C \end{cases} \tag{1b}$$

where L denotes the inductance, R presents the resistance, V_{in} stands for the external input voltage, C is the capacitance, v_o, v_C, i_L, i_C, r_L and r_C are the output voltage, capacitance voltage, inductive current, capacitance current, inductive impedance and capacitive reactance, respectively.

Define the state variable, output and input of the plant as: $x(t) = [i_L v_C]^T$, $z(t) = v_o$ and $u(t) = V_{in}$, respectively. Then, the state-space equation of the DC-DC converter can be characterized as

$$\begin{cases} \begin{cases} \dot{x}(t) = A_1 x(t) + B_1 u(t) \\ z(t) = C_1 x(t) \end{cases} & t \in (0, t_{\text{on}}] \\ \begin{cases} \dot{x}(t) = A_2 x(t) + B_2 u(t) \\ z(t) = C_2 x(t) \end{cases} & t \in (t_{on}, T] \end{cases} \tag{2}$$

where $A_1 = \begin{pmatrix} -\frac{r_L}{L} & 0 \\ 0 & -\frac{1}{C(R+r_C)} \end{pmatrix}$, $A_2 = \begin{pmatrix} -(\frac{r_L}{L} + \frac{r_C R}{L(R+r_C)}) & -\frac{R}{L(R+r_C)} \\ \frac{R}{C(R+r_C)} & -\frac{1}{C(R+r_C)} \end{pmatrix}$, $B_2 = B_1 = \begin{pmatrix} \frac{1}{L} \\ 0 \end{pmatrix}$, $C_1 = (0 \quad \frac{R}{R+r_C})$ and $C_2 = (\frac{r_C R}{R+r_C} \quad \frac{R}{R+r_C})$.

Remark 1. Generally, for aforementioned state equations in (2), the averaging model with state-space equation is employed, it can be characterized by: $\dot{x}(t) = \tau(t)[A_1 x(t) + B_1 u(t)] + (1 - \tau(t)) \times [A_2 x(t) + B_2 u(t)]$, where $\tau(t)$ denotes the switching function, and if $(0 \le t \le t_{\text{on}})$, then $\tau(t) = 1$; else $\tau(t) = 0$. Different from the averaging model, in this paper, the DC-DC converter is modeled by the semi-Markov stochastic model.

2.2. Modeling of DC-DC converter based on semi-Markov

In order to illustrate the semi-Markov model, the following three stochastic processes (SPs) are introduced [4]:

(1) The SP $\{\gamma(i)\} \in \Im = \{1, 2, ..., S\}$, where $\gamma(i)$ denotes the state of the plant at the i^{th} jump.
(2) The SP $\{t(i)\} \in R^+$, where $t(i)$ is the time at the i^{th}jump , with $t(0) = 0$.
(3) The SP $\{\varphi(i)\} \in R^+$, where $\varphi(i)$ represents the sojourn-time of state $\gamma(i)$ between the $(i-1)^{th}$ jump and i^{th} jump, and $\varphi(i) = t(i) - t(i-1)$ with $\varphi(0) = 0$.

Remark 2. In DC-DC converter, the switching process of switch operated at CCM is shown in Fig. 2, where T denotes one work period, t_{on} and t_{off} represent the on-time and off-time of the switch, respectively.

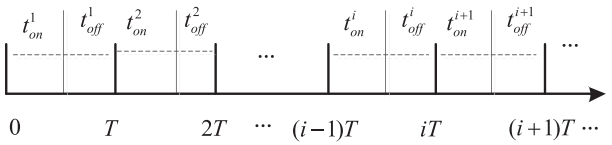

Fig. 2. Switching process in DC-DC converter operated at CCM.

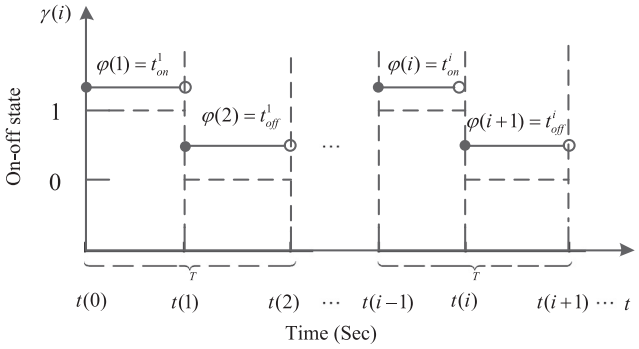

Fig. 3. The evolution of SPs $\gamma(i)$, $t(i)$ and $\varphi(i)$.

In this paper, the switching process of switch is modeled by the semi-Markov stochastic process. Meanwhile, consider the state-space equations in (2), a stochastic switched system is modeled, as following:

$$\begin{cases}\dot{x}(t)=A(\gamma(t))x(t)+B(\gamma(t))u(t)\\ z(t)=C(\gamma(t))x(t)\end{cases} \tag{3}$$

where $\{\gamma(t)\}_{t\geq 0}$ is a continuous-time and discrete-state stochastic process.

Remark 3. The evolution of SP $\{\gamma(t)\}_{t\geq 0}$ is shown in Fig. 3, it takes value in {0, 1}. $\gamma(t)$ is the switching signal and it obeys the semi-Markov distribution, the probability transitions are defined by

$$\Pr\{\gamma(t+\varphi)=s|\gamma(t)=l\}=\begin{cases}\lambda_{ls}(\varphi)\varphi+o(\varphi), \gamma(t) \text{ switching from } l \text{ to } s\\ 1+\lambda_{ll}(\varphi)\varphi+o(\varphi)\gamma(t) \text{ keeps at } l\end{cases} \tag{4}$$

where φ denotes the sojourn-time, and it is a random variable.

The evolution of SP $\{\varphi(t)\}_{t\geq 0}$ is shown in Fig. 3, it takes values in $\{\varphi(1), \varphi(2), ..., \varphi(i), ..\}$. $\lambda_{ls}(\varphi)$ is the transition rate from state l to state s if $l\neq s$, $\lambda_{ll}(\varphi)=-\sum_{s=1,s\neq l}^{N}\lambda_{ls}(\varphi)$, otherwise, $o(\varphi)$ is the high-order infinity about φ, i.e., $\lim_{\varphi\to 0} o(\varphi)/\varphi=0$.

Remark 4. As is shown in Fig. 3, the sojourn-time φ is the work time of the DC-DC converter in each state, and it will be return to 0 when the switch occurs moment. It is noted that the transition rate $\lambda_{ls}(\varphi)$ depends only on φ.

Remark 5. Different from the conventional state-space averaging model, in this paper, the sojourn-time φ is considered in the semi-Markov switched system, it will be more accurately to depict the dynamic behavior of the DC-DC converter.

Remark 6. Additionally, in practice system, on the one hand, as the change of the temperature and the aging of the system components, the value of resistance R will be changed. As a consequence, it will result in the parameter uncertainty of the plant, such as the resistance R change into $R+\Delta R$. On the other hand, the controlled system is inevitably deteriorated by external disturbance, such as the jump of input voltage.

As aforementioned analyzed, in this paper, considering the DC-DC converter as the semi-Markov switched system with the parameter uncertainty and external disturbance. Hence, the state-space equation can be rewritten as following:

$$\begin{cases}\dot{x}(t)=[A(\gamma(t))+\Delta A(\gamma(t))]x(t)+B(\gamma(t))u(t)+D(\gamma(t))d(t)\\ z(t)=C(\gamma(t))x(t)\end{cases} \tag{5}$$

where $d(t)$ denotes the jump of input voltage as the external disturbance, and $d(t)\in L_2[0,\infty)$, $D(\gamma(t))$ is the coefficient matrix with appropriate dimensions, $\Delta A(\gamma(t))$ represents the uncertainty of parameter which induced by the vary of the resistance R, and it satisfied the following relationship:

$$\Delta A(\gamma(t))=\Theta(\gamma(t))\vartheta(t)\mathrm{Y}(\gamma(t)) \tag{6}$$

where $\Theta(\gamma(t))$ and $\mathrm{Y}(\gamma(t))$ are the known matrices, and $\vartheta(t)$ is the unknown time-varying matrix with $\vartheta^T(t)\vartheta(t)\leq I$ is satisfied.

In what follows, for convenience, denoted $\gamma(t) = l$, then the system matrices in (5) can be written as: $A(l)$, $\Delta A(l)$, $B(l)$, $C(l)$ and $D(l)$.

3. Design of controller and stability analysis

In this subsection, firstly, the asynchronous controller will be designed. Then, the stability of the closed-loop plant will be analyzed.

3.1. Design of controller

In this paper, the following state feedback asynchronous controller will be designed:

$$u(t) = K(\alpha(t))x(t) \tag{7}$$

where $K(\alpha(t))$ denotes the controller gain to be designed, $\{\alpha(t)\}_{t \geq 0}$ is a stochastic process with $\alpha(t) \in \Re = \{1, 2, ..., F\}$, it is assumed that the following conditional probability is satisfied

$$\Pr\{\alpha(t) = q|\gamma(t) = l\} = \rho_{lq} \tag{8}$$

with $\sum_{q=1}^{F} \rho_{lq} = 1$.

Substitute (7) into (8), it can be obtained the following closed-loop system:

$$\dot{x}(t) = \left[\bar{A}(l) + B(l)K(q)\right]x(t) + D(l)d(t) \tag{9}$$

where $\bar{A}(l) = A(l) + \Delta A(l)$.

In order to discuss the stability of the stochastic closed-loop plant (9), the following definition will be given.

Definition 1. The closed-loop system (9) is stochastically stable with a $H\infty$ norm bound $\xi > 0$, if

(1) The closed-loop system (9) with $d(t) = 0$ is stochastically stable, i.e., for any initial condition $x(0) = x_0$, $\gamma(0) = \gamma_0$ and $t(0) = t_0$, there exists a constant $\Phi(x_0, \gamma_0, t_0) > 0$ such that

$$E\left[\int_0^{\infty} ||x(t)||^2 dt | x_0, \gamma_0, t_0\right] \leq \Phi(x_0, \gamma_0, t_0) \tag{10}$$

(2) Under the zero initial condition, that is, $x(0) \equiv 0$, for any $d(t) \in L_2[0, \infty)$, the following condition is satisfied:

$$\int_0^{\infty} z^T(t)z(t)dt \leq \xi^2 \int_0^{\infty} d^T(t)d(t)dt \tag{11}$$

3.2. Stability analysis

For the sake of analyzing the stability analysis of the closed-loop plant, the following results are given.

Theorem 1. *The closed-loop system (9) with $d(t) = 0$ is stochastically stable, if there exists the symmetric matrices $Q(l) > 0$, $Q(s) > 0$, $l, s \in \Im$, and matrices $K(q)$, $q \in \Re$, such that*

$$\sum_{s=1}^{N} \lambda_{ls}(\varphi)Q(s) + \sum_{q=1}^{F} \rho_{lq} Sym\{\tilde{A}^T(l)Q(l)\} < 0 \tag{12}$$

where $\tilde{A}(l) = \bar{A}(l) + B(l)K(q)$.

Proof. Constructing the following switched Lyapunov function for the closed-loop plant (9)

$$V(x(t), \gamma(t), t) = x^T(t)Q(\gamma(t))x(t) \tag{13}$$

Denote the infinitesimal operator [21]:

$$\dot{V}(x(t), \gamma(t), t) = \lim_{\eta \to 0} \frac{E[V(x(t+\eta), \gamma(t+\eta), t+\eta)|x(t), \gamma(t), t] - V(x(t), \gamma(t), t)}{\eta} \tag{14}$$

where η is a small number.

According to (13) and (14), it can be obtained that

$$\begin{aligned}\dot{V}(x(t), \gamma(t), t) = \lim_{\eta \to 0} \frac{1}{\eta} \Bigg[E\Bigg\{ &\sum_{s=1, s \neq l}^{N} \Pr\{\gamma(t+\eta) = s|\gamma(t) = l\} x^T(t+\eta)Q(s)x(t+\eta) \\ &+ \Pr\{\gamma(t+\eta) = l|\gamma(t) = l\} x^T(t+\eta)Q(l)x(t+\eta) \Bigg\} - x^T(t)Q(l)x(t) \Bigg]\end{aligned} \tag{15}$$

Define $\Psi_l(t)$ as the distribution function of the sojourn-time φ at state l. Then the (15) can be rewritten as

$$\dot{V}(x(t),\gamma(t),t) = \lim_{\eta\to 0}\frac{1}{\eta}E\Bigg[\sum_{s=1,s\neq l}^{N}\pi_{ls}\frac{[\Psi_l(\varphi+\eta)-\Psi_l(\varphi)]}{1-\Psi_l(\varphi)}x^T(t+\eta)Q(s)x(t+\eta) + \frac{1-\Psi_l(\varphi+\eta)}{1-\Psi_l(\varphi)}x^T(t+\eta)Q(l)x(t+\eta) - x^T(t)Q(l)x(t)\Bigg] \tag{16}$$

where π_{ls} is the probability intensity of the plant switching from state l to state s.

It is note that the first-order Taylor expansion of $x(t+\eta)$ in (16) is

$$x(t+\eta) = x(t) + \eta\dot{x}(t) + o(\eta) \tag{17}$$

where $o(\eta)$ is the high-order infinity about η, i.e., $\lim_{\varphi\to 0} o(\eta)/\eta = 0$.

Substitute (17) into (16), it can be obtained that

$$\dot{V}(x(t),\gamma(t),t) = \lim_{\eta\to 0}\frac{1}{\eta}E\Bigg[\sum_{s=1,s\neq l}^{N}\pi_{ls}\frac{\Psi_l(\varphi+\eta)-\Psi_l(\varphi)}{1-\Psi_l(\varphi)}\{x^T(t)Q(s)x(t)+2\eta x^T(t)Q(s)\dot{x}(t)+\eta^2\dot{x}^T(t)Q(s)\dot{x}(t)\} + \frac{1-\Psi_l(\varphi+\eta)}{1-\Psi_l(\varphi)}\{x^T(t)Q(l)x(t)+2\eta x^T(t)Q(l)\dot{x}(t)+\eta^2\dot{x}^T(t)Q(l)\dot{x}(t)\} - x^T(t)Q(l)x(t)\Bigg] \tag{18}$$

Duo to $\Psi_l(\varphi+\eta)-\Psi_l(\varphi)\to 0$ (when $\eta\to 0$) and $\lim_{\eta\to 0}\frac{1-\Psi_l(\varphi+\eta)}{1-\Psi_l(\varphi)} = 1$. Hence the (18) can be rewritten as

$$\dot{V}(x(t),\gamma(t),t) = E\Bigg[\sum_{s=1,s\neq l}^{N}\pi_{ls}\lim_{\eta\to 0}\frac{1}{\eta}\frac{[\Psi_l(\varphi+\eta)-\Psi_l(\varphi)]}{1-\Psi_l(\varphi)}x^T(t)Q(s)x(t) - \lim_{\eta\to 0}\frac{1}{\eta}\frac{\Psi_l(\varphi+\eta)-\Psi_l(\varphi)}{1-\Psi_l(\varphi)}x^T(t)Q(l)x(t) + 2x^T(t)Q(l)\dot{x}(t)\Bigg] \tag{19}$$

Define $\lambda_l(\varphi)$ and $f_l(\varphi)$ as the transition rate and the probability density function of the stochastic sojourn-time φ in state l, respectively. Therefore

$$\lim_{\eta\to 0}\frac{1}{\eta}\frac{\Psi_l(\varphi+\eta)-\Psi_l(\varphi)}{1-\Psi_l(\varphi)} = \frac{1}{1-\Psi_l(\varphi)}\lim_{\eta\to 0}\frac{\Psi_l(\varphi+\eta)-\Psi_l(\varphi)}{\eta} = \frac{f_l(\varphi)}{1-\Psi_l(\varphi)} = \lambda_l(t) \tag{20}$$

Considering the Eq. (20), it can be deduced that

$$\dot{V}(x(t),\gamma(t),t) = E\Bigg[\sum_{s=1,s\neq l}^{N}\pi_{ls}\lambda_l(\varphi)x^T(t)Q(s)x(t) - \lambda_l(t)x^T(t)Q(l)x(t) + 2x^T(t)Q(l)\dot{x}(t)\Bigg] \tag{21}$$

Let $\lambda_{ls}(\varphi) = \pi_{ls}\lambda_l(\varphi), l\neq s$ and $\lambda_{ll}(\varphi) = -\sum_{s=1,s\neq l}^{N}\lambda_{ls}(\varphi)$, then the (21) becomes

$$\dot{V}(x(t),\gamma(t),t) = E\Bigg[x^T(t)\Bigg(\sum_{s=1}^{N}\lambda_{ls}(\varphi)Q(s)\Bigg)x(t) + 2x^T(t)Q(l)\dot{x}(t)\Bigg] \tag{22}$$

Substitute (9) into (22) yields,

$$\dot{V}(x(t),\gamma(t),t) = x^T(t)\Bigg(\sum_{s=1}^{N}\lambda_{ls}(\varphi)Q(s) + \sum_{q=1}^{F}\rho_{lq}Sym\{\tilde{A}^T(l)Q(l)\}\Bigg)x(t) = x^T(t)\Omega(l,s,t)x(t) \tag{23}$$

where $\Omega(l,s,t) = \sum_{s=1}^{N}\lambda_{ls}(\varphi)Q(s) + \sum_{q=1}^{F}\rho_{lq}Sym\{\tilde{A}^T(l)Q(l)\}$.

According to (12), it can be deduced that

$$\Omega(l,s,t) < I\max_{l\in\Im,t}\{\lambda_{\max}(\Omega(l,s,t))\} < 0 \tag{24}$$

Hence,

$$\begin{aligned} &E[V(x(t),\gamma(t),t)]-V(x_0,\gamma_0,t_0)\\ &=E\left[\int_0^t \dot{V}(x(\kappa),\gamma(\kappa),\kappa)d\kappa|x_0,\gamma_0,t_0\right]\\ &=E\left[\int_0^t x^T(\kappa)\Omega(l,s,\kappa)x(\kappa)d\kappa|x_0,\gamma_0,t_0\right]\\ &\le \max_{l\in\Im,t}\{\lambda_{max}(\Omega(l,s,t))\}E\left[\int_0^t ||x(\kappa)||^2 d\kappa|x_0,\gamma_0,t_0\right]<0 \end{aligned} \tag{25}$$

The (25) indicates that

$$V(x_0,\gamma_0,t_0)\ge -\max_{l\in\Im,t}\{\lambda_{max}(\Omega(l,s,t))\}E\left[\int_0^t ||x(\kappa)||^2 d\kappa|x_0,\gamma_0,t_0\right]>0 \tag{26}$$

Furthermore,

$$-\frac{V(x_0,\gamma_0,t_0)}{\max\limits_{l\in\Im,t}\{\lambda_{max}(\Omega(l,s,t))\}}\ge E\left[\int_0^t ||x(\kappa)||^2 d\kappa|x_0,\gamma_0,t_0\right]>0$$

When $t\to\infty$, it can be obtained that

$$E\left[\int_0^t ||x(\kappa)||^2 d\kappa|x_0,\gamma_0,t_0\right]\le \Phi(x_0,\gamma_0,t_0) \tag{27}$$

where $\Phi(x_0,\gamma_0,t_0)=-\frac{V(x_0,\gamma_0,t_0)}{\max\limits_{l\in\Im,t}\{\lambda_{\max}(\Omega(l,s,t))\}}$.

According to Definition 1, the (27) indicates that the closed-loop system (9) with $d(t)=0$ is stochastically stable. This completes the proof. □

Furthermore, we will investigate the $H\infty$ damping performance for the disturbance $d(t)\neq 0$. Firstly, in order to deal with the uncertainty, the following lemma is given.

Lemma 1 [13]: If $\vartheta^T(t)\vartheta(t)\le I$, then there exists constant matrices $\aleph$ and $\Re$, and the scalar $\varepsilon>0$ such that

$$\Re\vartheta(t)\aleph+\aleph^T\vartheta^T(t)\Re^T\le\varepsilon\Re\Re^T+\varepsilon^{-1}\aleph^T\aleph \tag{28}$$

Theorem 2. *Given a scalar $\xi>0$, the closed-loop plant (9) is stochastically stable with a $H\infty$ damping index ξ, if there exists the symmetric matrices $Q(l)>0$, $Q(s)>0$, $l,s\in\Im$, matrices $K(q)$, $q\in\Re$, and a set of scalars $\varepsilon_l>0$, $l\in\Im$, such that*

$$\begin{pmatrix} \Omega_{11}(l,s,t) & Q(l)D(l) & C^T(l) & \Upsilon^T(l)\\ * & -\xi^2 I & 0 & 0\\ * & * & -I & 0\\ * & * & * & -\varepsilon_l^{-1}I \end{pmatrix}<0 \tag{29}$$

where

$$\Omega_{11}(l,s,t)=\sum_{s=1}^{N}\lambda_{ls}(\varphi)Q(s)+Sym\{A^T(l)Q(l)\}+\sum_{q=1}^{F}\rho_{lq}Sym\{(B(l)K(q))^TQ(l)\}+\varepsilon_l Q(l)\Theta(l)\Theta^T(l)Q(l).$$

Proof. Firstly, define

$$J=\int_0^\infty\{z^T(t)z(t)-\xi^2 d^T(t)d(t)\}dt \tag{30}$$

Under the zero initial condition, the following condition is satisfied for any nonzero $d(t)\in L_2[0,\infty)$

$$J\le\int_0^\infty\{\dot{V}(x(t),\gamma(t),t)+z^T(t)z(t)-\xi^2 d^T(t)d(t)\}dt \tag{31}$$

Let $\bar{x}(t)=[x(t)d(t)]^T$, according to Theorem 1, it can be derived that

$$\begin{aligned} J\le\int_0^\infty\Bigg\{&x^T(t)\left(\sum_{s=1}^{N}\lambda_{ls}(\varphi)Q(s)+\sum_{q=1}^{F}\rho_{lq}Sym\{\tilde{A}^T(l)Q(l)\}\right)x(t)\\ &+2x^T(t)Q(l)D(l)d(t)+x^T(t)C^T(l)C(l)x(t)-\xi^2 d^T(t)d(t)\Bigg\}dt \end{aligned}$$

$$= \int_0^\infty \bar{x}^T(t)\begin{pmatrix} \Psi' & Q(l)D(l) \\ D^T(l)Q(l) & -\xi^2 I \end{pmatrix}\bar{x}(t)dt \tag{32}$$

where $\Psi' = \sum_{s=1}^{N}\lambda_{ls}(\varphi)Q(s) + \sum_{q=1}^{F}\rho_{lq}Sym\{\tilde{A}^T(l)Q(l)\} + C^T(l)C(l)$.

Combining with the (6) yields

$$\sum_{q=1}^{F}\rho_{lq}Sym\{\tilde{A}^T(l)Q(l)\} = \sum_{q=1}^{F}\rho_{lq}\mathrm{Sym}\{(B(l)K(q))^T Q(l)\} + Sym\{A^T(l)Q(l)\} + [Q(l)\Theta(l)\vartheta(t)\Upsilon(l)]^T + Q(l)\Theta(l)\vartheta(t)\Upsilon(l) \tag{33}$$

Using the Lemma 1, the (33) becomes

$$\sum_{q=1}^{F}\rho_{lq}Sym\{\tilde{A}^T(l)Q(l)\} \le \sum_{q=1}^{F}\rho_{lq}Sym\{(B(l)K(q))^T Q(l)\} + Sym\{A^T(l)Q(l)\} + \varepsilon_l Q(l)\Theta(l)\Theta^T(l)Q(l) + \varepsilon_l^{-1}\Upsilon^T(l)\Upsilon(l) \tag{34}$$

Combining with (32), (33) and (34), it can be derived that

$$J \le \int_0^\infty \bar{x}^T(t)\tilde{\Psi}\bar{x}(t)dt \tag{35}$$

where

$$\tilde{\Psi} = \begin{pmatrix} \tilde{\Psi}' + \tilde{\Psi}'' + \tilde{\Psi}''' & Q(l)D(l) \\ D^T(l)Q(l) & -\xi^2 I \end{pmatrix},$$

$$\tilde{\Psi}' = \sum_{s=1}^{N}\lambda_{ls}(t)Q(s) + C^T(l)C(l),$$

$$\tilde{\Psi}'' = \sum_{q=1}^{F}\rho_{lq}\mathrm{Sym}\{(B(l)K(q))^T Q(l)\} + Sym\{A^T(l)Q(l)\},$$

$$\tilde{\Psi}''' = \varepsilon_l Q(l)\Theta(l)\Theta^T(l)Q(l) + \varepsilon_l^{-1}\Upsilon^T(l)\Upsilon(l).$$

Furthermore, using the Shur complement, the matrix $\tilde{\Psi}$ in (35) can be easily transformed into the matrix in (29). Hence, the inequality in (29) indicates that $J \le \int_0^\infty \bar{x}^T(t)\tilde{\Psi}\bar{x}(t)dt < 0$, that is, $\int_0^\infty z^T(t)z(t)dt \le \xi^2\int_0^\infty d^T(t)d(t)dt$ for any nonzero $d(t) \in L_2[0,\infty)$. According to the Definition 1, the closed-loop system (9) is stochastically stable with a $H\infty$ damping index ξ. This finishes the proof. □

Furthermore, for the sake of solving the controller gains, the following stability condition based on linear matrix inequality is given.

Theorem 3. *For given scalars $\xi > 0$ and $\varepsilon_l > 0$, $l \in \Im$, the closed-loop plant (9) is stochastically stable with a $H\infty$ damping index ξ, if there exists the symmetric and positive definite matrices $Q(l)$, $\Gamma(l)$, $l \in \Im$, and matrices $M(q)$, $q \in \Re$ such that the following inequality is satisfied*

$$\begin{pmatrix} \tilde{\Omega}_{11} & D(l) & \Gamma(l)C^T(l) & \Gamma(l)\Upsilon^T(l) & \Theta(l) & \tilde{\Gamma}(l) \\ * & -\xi^2 I & 0 & 0 & 0 & 0 \\ * & * & -I & 0 & 0 & 0 \\ * & * & * & -\varepsilon_l^{-1}I & 0 & 0 \\ * & * & * & * & -\varepsilon_l I & 0 \\ * & * & * & * & * & -\tilde{Q} \end{pmatrix} < 0 \tag{36}$$

where $\tilde{\Omega}_{11} = Sym\{\Gamma(l)A^T(l)\} + \sum_{q=1}^{F}\rho_{lq}Sym\{M^T(q)B^T(l)\} + \bar{\lambda}_{ll}\Gamma(l)$, $\tilde{\Gamma}(l) = [\sqrt{\bar{\lambda}_{l,1}}\cdots\sqrt{\bar{\lambda}_{l,l-1}}\sqrt{\bar{\lambda}_{l,l+1}}\cdots\sqrt{\bar{\lambda}_{l,N}}]\Gamma(l)$, $\tilde{Q} = diag\{\Gamma(1),\ldots,\Gamma(l-1),\Gamma(l+1),\ldots,\Gamma(N)\}$ and $\bar{\lambda}_{ls} = E\{\lambda_{ls}(\varphi)\} = \int_0^\infty \lambda_{ls}(\varphi)f_l(\varphi)d\varphi$.

The controller gain can be solved by

$$K(q) = M(q)\Gamma^{-1}(l) \tag{37}$$

Proof. Firstly, define $\Gamma(l) = Q^{-1}(l)$ and $M(q) = K(q)\Gamma(l)$, then pre- and postmultiplying inequality (29) by $diag\{\Gamma(l), I, I, I\}$, it can be derived that

$$\begin{pmatrix} \bar{\Omega}_{11}(l,s,t) & D(l) & \Gamma(l)C^T(l) & \Gamma(l)\Upsilon^T(l) \\ * & -\xi^2 I & 0 & 0 \\ * & * & -I & 0 \\ * & * & * & -\varepsilon_l^{-1} I \end{pmatrix} < 0 \tag{38}$$

where

$$\bar{\Omega}_{11}(l,s,t) = \bar{\lambda}_{ll}\Gamma(l) + \Gamma(l)\left(\sum_{s=1,s\neq l}^{N} \bar{\lambda}_{ls} Q(s)\right)\Gamma(l) + Sym\left\{\Gamma(l)A^T(l)\right\} + \sum_{q=1}^{F} \rho_{lq} Sym\left\{M^T(q)B^T(l)\right\} + \varepsilon_l \Theta(l)\Theta^T(l).$$

Using the Shur complement and some changes of variables, the matrix in (38) can be transformed into the matrix in (36). This completes the proof. □

4. Simulations and experiments

4.1. Numerical simulations

In this subsection, in order to prove the superiority of the designed method, a boost DC-DC converter is considered, according to [11], the parameters of the plant are: $r_C = 0.1\Omega$, $r_L = 0.1\Omega$, $L = 95 \times 10^{-6}H$, $V_o = 80V$, $C = 300 \times 10^{-6}F$, $P_o = 500W$ and $R = V_o^2/P_o = 12.8\Omega$. Substituting them into states space equations (2) yields

$$A_1 = \begin{pmatrix} -1052.6316 & 0 \\ 0 & -258.3979 \end{pmatrix}, B_1 = \begin{pmatrix} 10526.3158 \\ 0 \end{pmatrix}, C_1 = \begin{pmatrix} 0 \\ 0.9922 \end{pmatrix}^T$$

$$A_2 = \begin{pmatrix} -2097.0525 & -10444.2105 \\ 3307.4935 & -258.3979 \end{pmatrix}, B_2 = \begin{pmatrix} 10526.3158 \\ 0 \end{pmatrix}, C_2 = \begin{pmatrix} 0.0992 \\ 0.9922 \end{pmatrix}^T,$$

The uncertainty term $\Delta A(\gamma(t)) = \Theta(\gamma(t))\vartheta(t)\Upsilon(\gamma(t))$ are set as:

$$\Theta_1 = \Theta_2 = \begin{pmatrix} 0.1 & 0.1 \end{pmatrix}^T, \Upsilon_1 = \Upsilon_2 = \begin{bmatrix} 0.1 & 0.1 \end{bmatrix} \text{and } \vartheta_1(t) = \vartheta_2(t) = 2.5\sin(t)$$

The disturbance term $D(\gamma(t))d(t)$ are set as: $D_1 = D_2 = \begin{pmatrix} 0.04 & 0.01 \end{pmatrix}^T$ and $d(t) = 1.5\cos(t)$. It is noticed that there are only two operation states in each sampling period (that is switch on and switch off). Hence, the transition intensity satisfied: $\pi_{ls} = 1$ for $l \neq s$ and $\pi_{ll} = 0$. Assuming that the sojourn time of the switch obeys the Weibull distribution at each state. The transition rate function from mode l is: $\lambda_l(\varphi) = (\beta/\alpha^\beta)\varphi^{\beta-1}$ where β shows the shape parameter of the Weibull distribution and α is the scale parameter. In this paper, for $l = 1$, let $\alpha = 1$ and $\beta = 2$, when $l = 2$, let $\alpha = 1$ and $\beta = 3$. Then the transition rate matrix can be obtained:

$$[\lambda_{ls}(\varphi)] = \begin{bmatrix} -2\varphi & 2\varphi \\ 3\varphi^2 & -3\varphi^2 \end{bmatrix}.$$

Furthermore, the expectation value can derived by $E\{\lambda_{ls}(\varphi)\} = \int_0^\infty \lambda_{ls}(\varphi) f_l(\varphi) d\varphi$, that is

$$\bar{\lambda}_{ls} = E\{[\lambda_{ls}(\varphi)]\} = \begin{bmatrix} -1.7725 & 1.7725 \\ 2.7082 & -2.7082 \end{bmatrix}.$$

The parameters of the matrix $[\rho_{lq}]$ in asynchronous controller is set to be

$$[\rho_{lq}] = \begin{bmatrix} 0.3 & 0.7 \\ 0.8 & 0.2 \end{bmatrix}.$$

The $H\infty$ damping index $\xi = 16$, the parameters $\varepsilon_1 = \varepsilon_2 = 0.01$. The simulations time is set to be 10 s, and the sampling period is 0.05 s. The initial condition is set: $x(0) = [0.60.8]^T$, $\gamma(1) = 1$ and $\alpha(1) = 2$. According to Theorem 3, the controller gains can be obtained as follows:

$$K_{11} = [0.0558 - 0.0003],\ K_{12} = [0.1186 - 0.0003],\ K_{21} = [0.1997 - 2.6722] \text{ and } K_{22} = [0.0502 - 0.6681]$$

The simulation results are shown in Figs. 4–6. Among which, Fig. 4 depicts the switching process of the variable $\gamma(t)$ and $\alpha(t)$, where the sojourn-times $\varphi(l)$ of switch on and switch off are stochastic, and the lower and upper bound of the sojourn-time are 1.0 s and 2.5 s, respectively. When $\gamma(t) = 1$, the probabilities are 0.3 and 0.7 for $\alpha(t) = 1$ and $\alpha(t) = 2$. Otherwise, the probabilities are 0.8 and 0.2 for $\alpha(t) = 1$ and $\alpha(t) = 2$, respectively. Fig. 5 gives the trajectories of the states x_1 and x_2 under designed asynchronous control strategy, it can be seen that both states can converge to the equilibrium point at about 1.0 s. Fig. 6 presents the trajectories of the input under asynchronous control strategy.

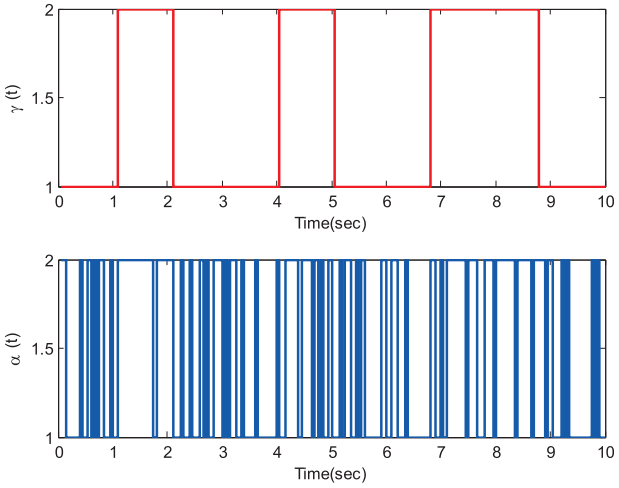

Fig. 4. Switching process of the variable $\gamma(t)$ and $\alpha(t)$.

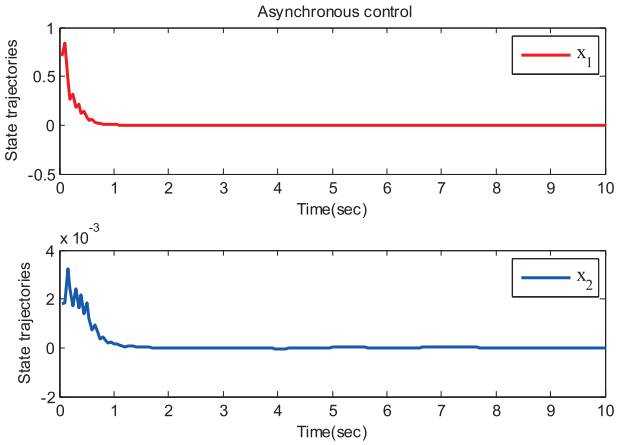

Fig. 5. Trajectories of the states under asynchronous control.

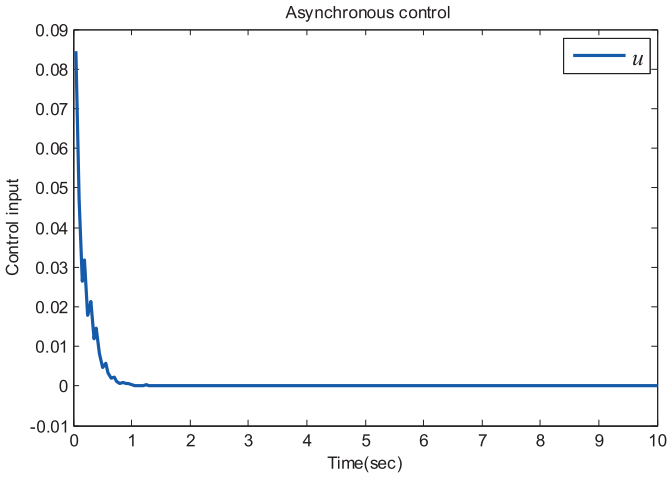

Fig. 6. Trajectories of the input under asynchronous control.

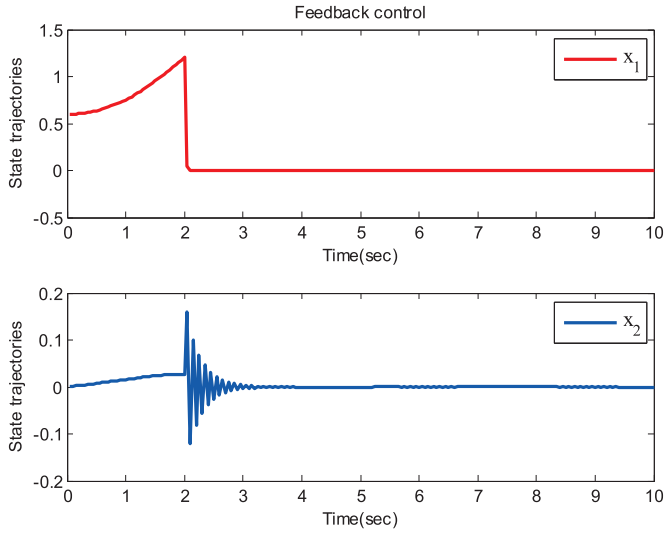

Fig. 7. Trajectories of the states under feedback control.

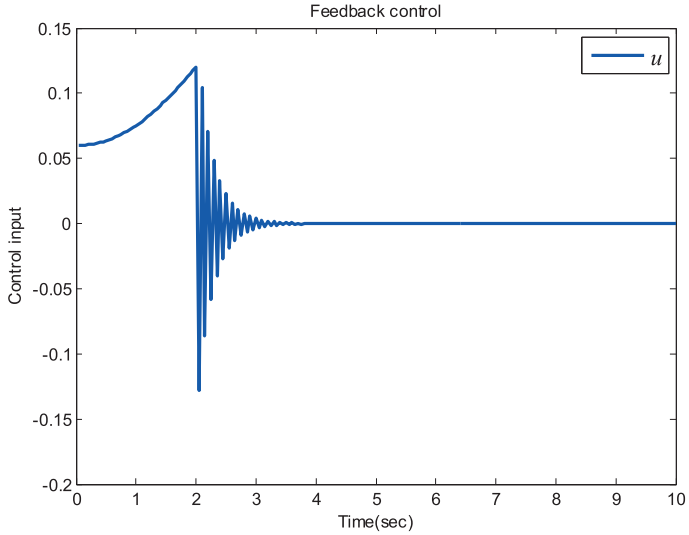

Fig. 8. Trajectories of the input under feedback control.

Furthermore, in order to illustrate the effectiveness of designed method, the traditional feedback control approach is carried out as comparison, the parameters and initial conditions are set as same as above. The simulation results are shown in Figs. 7 and 8. The trajectories of the states under traditional feedback control are given in Fig. 7. It takes about 3.0 s for the states converge to the equilibrium point. Fig. 8 plots the trajectories of the input under traditional feedback control. Additionally, comparing the designed asynchronous control strategy with the traditional feedback control approach, we can conclude that the convergence of proposed asynchronous control is faster than the traditional feedback control.

4.2. Practical experiment

In this subsection, the simulations of boost DC-DC converter are carried out on Dspace. As is shown in Fig. 9, the computer host and Dspace are linked by network. Firstly, the Dspace executes the compute, and then return the results to the control desk. And also, the operation results can be display by scope.

Remark 7. In the boost DC-DC converter, the switch is stochastic switching, and the times of switch on t_{on} and switch offt_{off} are time-varying, that is the state transition rate is time-varying. Hence, it is very reasonable to employ the semi-Markov stochastic process to model the converter. Additionally, the asynchronous phenomenon is existed between controller nodes and the converter duo to some components fault, communication delay, and disturbance, and so on. Therefore, in this paper, the asynchronous strategy is designed to control converter.

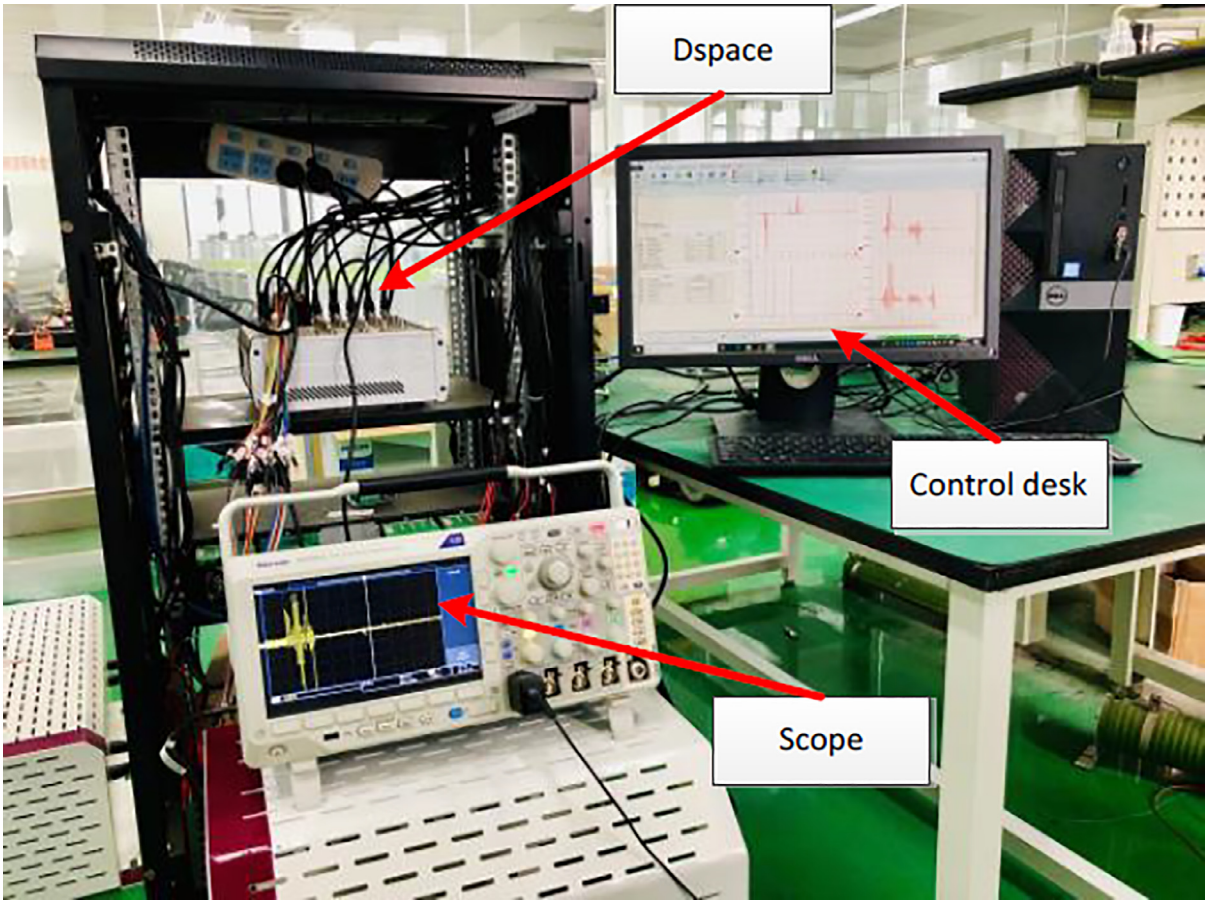

Fig. 9. DC-DC converter simulation based on Dspace.

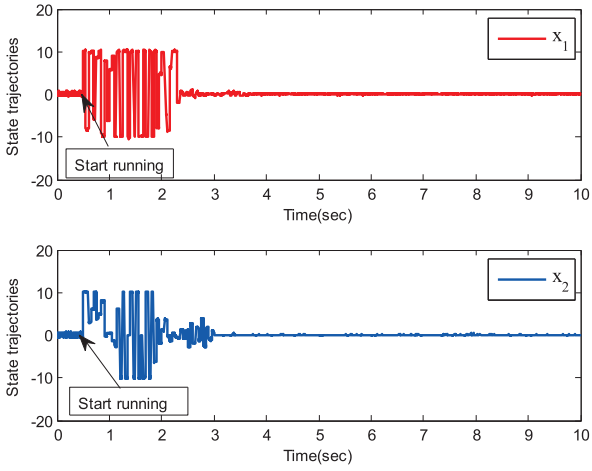

Fig. 10. Trajectories of the states under asynchronous control.

In the simulations, the parameters of the DC-DC converter are set as same as Part A. The initial condition is set: $x(0) = [0.81.2]^{\mathrm{T}}$, $\gamma(1) = 1$, and $\alpha(1) = 1$. The uncertainty term and the disturbance term are set as: $\vartheta_1(t) = \vartheta_2(t) = 5.5\cos(4t) \times \sin(2t)$ and $d(t) = 6.5[\cos(4t) + \sin(6t)]$, respectively. Other parameters are set as same as above.

The simulations are started at 0.5 s. The simulation results are shown as follows. Fig. 10 presents the trajectories of the states designed asynchronous control strategy. Seen from the results, it can be seen that both states are unstable at begin of the system starts running. And also it takes about 2.5 s for the states to reach the equilibrium point. Fig. 11 gives

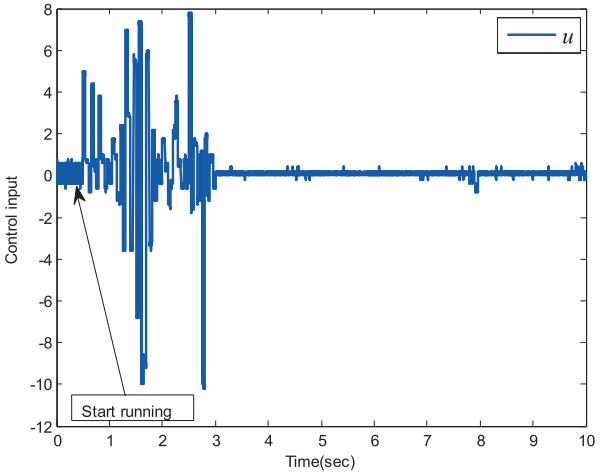

Fig. 11. Trajectories of the input under asynchronous control.

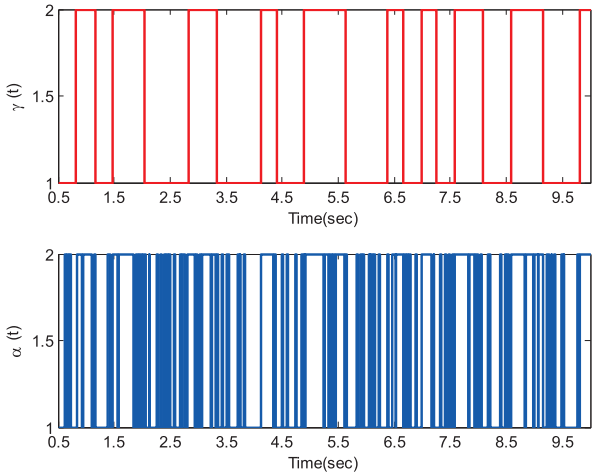

Fig. 12. Switching process of the variables $\gamma(t)$ and $\alpha(t)$.

the trajectories of the control input. It can be seen that the control input occurs violent shaking after the system starts running, and there still exists some minor oscillation even the control input reaches the equilibrium point. Fig. 12 shows the switching process of the variables $\gamma(t)$ and $\alpha(t)$. It can be seen that the switching signals begin working at 0.5 s duo to the system starts running at that time. In Fig. 12, the variable $\gamma(t)$ denotes the sojourn-time which is random, with the lower and upper bound are 0.325 s and 1.25 s, respectively. The variable $\alpha(t)$ is the index signal of the asynchronous controller. Both variables $\gamma(t)$ and $\alpha(t)$ are connected by the conditional probability.

5. Conclusion

In this paper, the problem of modeling and control of boost DC-DC converter is studied. In which, a semi-Markov switched model is established and an asynchronous control strategy is proposed for the DC-DC converter. Firstly, considering the change of resistance parameter and the jump of input voltage in the DC-DC converter, an S-MJS with uncertainty and external disturbance is modeled. Additionally, in order to accurately characterize the dynamic behavior of the converter, the sojourn-time of the switch is considered in the model. Secondly, a state feedback asynchronous strategy is designed for achieving the stability of the system. Thirdly, the stability conditions of the closed-loop plant with a prescribed H_∞ index factor are given and the controller gains are solved. Finally, in order to prove the effectiveness of presented control strategies, a numerical simulation and a practical experiment are executed. In the further work, the DC-DC converter jumping systems with the general constrained switching signals, such as dwell time and average dwell time will be studied.

Acknowledgements

This work was supported by the National Natural Science Foundation of China under grant (61903064 and 61973331), the China Postdoctoral Science Foundation funded project under grant (2019M663479), the Fundamental Research Funds for the Central Universities under grant (ZYGX2019J058), the National Key Research and Development Plan Programs of China under grant (2018YFB0106101), and the Postdoctoral Fund Project of University of Electronic Science and Technology of China(UESTC) under grant (Y030190236010162000).

References

[1] H. Behjati, L. Niu, A. Davoudi, P. Chapman, Alternative time-invariant multi-frequency modeling of PWM DC-DC converters, IEEE Trans. Circuits Syst. 60 (11) (2013) 3069–3079.
[2] S. Dong, M. Fang, S. Chen, Extended dissipativity asynchronous static output feedback control of Markov jump systems, Inf. Sci. 514 (2020) 275–287.
[3] S. Dong, Z. Wu, H. Su, P. Shi, H. Karimi, Asynchronous control of continuous-time nonlinear Markov jump systems subject to strict dissipativity, IEEE Trans. Automat. Contr. 64 (3) (2019) 1250–1256.
[4] J. Huang, Y. Shi, Stochastic stability and robust stabilization of semi-Markov jump linear systems, Int. J. Robust Nonlinear Control 23 (2013) 2028–2043.
[5] J. Huang, Y. Shi, Stochastic stability of semi-Markov jump linear systems: an LMI approach, in: Proceedings of the Fiftieth IEEE Conference on Decision and Control and European Control Conference, 2011, pp. 4668–4673.
[6] B. Jiang, H. Karimi, Y. Kao, C. Gao, Reduced-order adaptive sliding mode control for nonlinear switching semi-Markovian jump delayed systems, Inf. Sci. 477 (2019) 334–348.
[7] B. Jiang, Y. Kao, C. Gao, X. Yao, Passification of uncertain singular semi-Markovian jump systems with actuator failures via sliding mode approach, IEEE Trans. Automat. Contr. 62 (8) (2017) 4138–4143.
[8] S. Kim, Output voltage-tracking controller with performance recovery property for DC/DC boost converters, IEEE Trans. Control Syst. Technol. 27 (3) (2019) 1301–1307.
[9] M. Li, Y. Chen, W. He, X. Li, Adaptive tracking control for networked control systems of intelligent vehicle, Inf. Sci. 503 (2019) 493–507.
[10] X. Li, X. Ruan, Q. Jin, M. Sha, C. Tse, Approximate discrete-time modeling of DC–DC converters with consideration of the effects of pulse width modulation, EEE Trans. Power Electron. 33 (8) (2018) 7071–7082.
[11] X. Li, X. Ruan, Q. Jin, M. Sha, C. Tse, Small-signal models with extended frequency range for DC–DC converters with large modulation ripple amplitude, IEEE Trans. Power Electron. 33 (9) (2018) 8151–8163.
[12] Z. Ning, L. Zhang, J. Lam, Stability and stabilization of a class of stochastic switching systems with lower bound of sojourn time, Automatica 92 (2018) 18–28.
[13] L. Qiu, Y. Shi, F. Yao, G. Xu, B. Xu, Network-based robust H_2/H_∞ control for linear systems with two-channel random packet dropouts and time delays, IEEE Trans. Cybern. 45 (8) (2015) 1450–1462.
[14] B. Saporta, E. Costa, Approximate Kalman–Bucy filter for continuous- time semi-Markov jump linear systems, IEEE Trans. Automat. Contr. 61 (8) (2016) 2035–2048.
[15] H. Shen, F. Li, S. Xu, V. Sreeram, Slow state variables feedback stabilization for semi-markov jump systems with singular perturbations, IEEE Trans. Automat. Contr. 63 (8) (2018) 2709–2714.
[16] Y. Shen, Z. Wu, P. Shi, Z. Shu, H. Karimi, H_∞ control of Markov jump time-delay systems under asynchronous controller and quantizer, Automatica 99 (2019) 352–360.
[17] P. Shi, M. Liu, L. Zhang, Fault-tolerant sliding-mode-observer synthesis of Markovian jump systems using quantized measurements, IEEE Trans. Ind. Electron. 62 (9) (2015) 5910–5918.
[18] J. Song, Y. Niu, Y. Zou, Asynchronous sliding mode control of Markovian jump systems with time-varying delays and partly accessible mode detection probabilities, Automatica 93 (2018) 33–41.
[19] X. Song, M. Wang, B. Zhang, S. Song, Event-triggered reliable H_∞ fuzzy filtering for nonlinear parabolic PDE systems with Markovian jumping sensor faults, Inf. Sci. 510 (2020) 50–69.
[20] Y. Wei, J. Park, J. Qiu, L. Wu, H. Jung, Sliding mode control for semi-Markovian jump systems via output feedback, Automatica 81 (2017) 133–141.
[21] Z. Xu, H. Su, P. Shi, Z. Wu, Asynchronous H_∞ control of semi-Markov jump linear systems, Appl. Math. Comput. 349 (2019) 270–280.
[22] R. Yang, W. Zheng, H∞ filtering for discrete-time 2-D switched systems: an extended average dwell time approach, Automatica 98 (2018) 302–313.
[23] L. Zhang, Y. Leng, P. Colaneri, Stability and stabilization of discrete-time semi-Markov jump linear systems via semi-Markov kernel approach, IEEE Trans. Automat. Contr. 61 (2) (2016) 503–508.
[24] L. Zhang, G. Li, Controller design for discrete-time hybrid linear parameter-varying systems with semi-Markov mode switching, J. Franklin Inst. 355 (2018) 7056–7071.
[25] L. Zhang, T. Yang, P. Colaneri, Stability and stabilization of semi-Markov jump linear systems with exponentially modulated periodic distributions of sojourn time, IEEE Trans. Automat. Contr. 62 (6) (2017) 2870–2885.
[26] Y. Zhu, and W. Zheng, Multiple Lyapunov functions analysis approach for discrete-time switched piecewise-affine systems under dwell-time constraints, IEEE Trans. Autom. Control, DOI: 10.1109/TAC.2019.2938302.